

8-1999

Macrosegregation Caused by Thermosolutal Convection During Directional Solidification of Pb-Sb Alloys

S. N. Ojha
Banaras Hindu University

G. L. Ding
Cleveland State University

Y. Lu
Cleveland State University

J. Reye
Cleveland State University

Surendra N. Tewari

Download this State University works at: https://engagedscholarship.csuohio.edu/encbe_facpub

 Part of the [Materials Science and Engineering Commons](#)

How does access to this work benefit you? Let us know!

Original Citation

Ojha, S.N., Ding, G., Lu, Y., Reye, J., & Tewari, S.N. (1999). Macrosegregation Caused by Thermosolutal Convection During Directional Solidification of Pb-Sb Alloys. *Metallurgical and Materials Transactions A: Physical Metallurgy and Materials Science* **30**, 2167-2171.

Repository Citation

Ojha, S. N.; Ding, G. L.; Lu, Y.; Reye, J.; and Tewari, Surendra N., "Macrosegregation Caused by Thermosolutal Convection During Directional Solidification of Pb-Sb Alloys" (1999). *Chemical & Biomedical Engineering Faculty Publications*. 23.

https://engagedscholarship.csuohio.edu/encbe_facpub/23

This Article is brought to you for free and open access by the Chemical & Biomedical Engineering Department at EngagedScholarship@CSU. It has been accepted for inclusion in Chemical & Biomedical Engineering Faculty Publications by an authorized administrator of EngagedScholarship@CSU. For more information, please contact library.es@csuohio.edu.

Macroseggregation Caused by Thermosolutal Convection during Directional Solidification of Pb-Sb Alloys

S.N. OJHA, G. DING, Y. LU, J. REYE, and S.N. TEWARI

Pb-2.2 and 5.8 wt pct Sb alloys were directionally solidified with a positive thermal gradient of 140 K cm^{-1} at growth speeds ranging from 0.8 to $30 \mu\text{m s}^{-1}$, and then quenched to retain the mushy-zone morphology. Chemical analysis along the length of the directionally solidified portion and in the quenched melt ahead of the dendritic array showed extensive longitudinal macrosegregation. Cellular morphologies growing at smaller growth speeds are associated with larger amounts of macrosegregation as compared with the dendrites growing at higher growth speeds. Convection is caused, mainly, by the density inversion in the overlying melt ahead of the cellular/dendritic array because of the antimony enrichment at the array tip. Mixing of the interdendritic and bulk melt during directional solidification is responsible for the observed longitudinal macrosegregation.

I. INTRODUCTION

MACROSEGREGATION during directional solidification with a dendritic liquid-solid interface morphology has been extensively investigated because of the commercial importance of superalloy components. Macroseggregation, *i.e.*, solutal inhomogeneity over length scales larger than primary dendrite spacing, results from convection in the mushy zone. Convection can be caused by solidification shrinkage, sinking or floating of broken-off dendrite segments, and the temperature- or composition-induced melt density inversion. It can produce localized segregation ("channel segregates or freckles")^[1,2,3] clustering or steeping of dendrites across the liquid-solid interface,^[4] or a systematic variation in solute content along the length of the directionally solidified ingot.^[5,6,7] We had earlier examined macrosegregation along the length of the directionally solidified Pb-Sn alloys as part of a program to study the influence of convection on the dendritic and mushy-zone morphology.^[5,6,7] In this article, we examine the macrosegregation caused by solutal buildup at the dendrite tips under thermally stable and solutally unstable directional solidification conditions for two hypoeutectic Pb-Sb alloys containing 2.2 and 5.8 wt pct Sb, respectively. Solute content of the first alloy is less than the terminal solid solubility limit of antimony in lead (3.5 wt pct Sb), whereas that of the second alloy is more. The second alloy, containing 5.8 wt pct Sb, is therefore expected to have a more permeable mushy zone compared to that of the alloy containing 2.2 wt pct Sb.

II. EXPERIMENTAL PROCEDURE

Approximately 24- to 30-cm-long Pb-Sb feedstock samples were obtained by induction melting a charge (lead, 99.99 pct purity and antimony, 99.999 pct purity) under an argon atmosphere in a graphite crucible and pushing the

melt into evacuated quartz tubes (0.7-cm i.d.) with the help of argon pressure. The cast Pb-2.2 wt pct Sb and Pb-5.8 wt pct Sb feedstock cylinders were extracted and placed into the quartz directional solidification ampoule (0.7-cm i.d., 70-cm long). The quartz ampoule contained two Chromel-Alumel thermocouples (0.01-cm-diameter wires kept in closed-end silica capillaries, of 0.06-cm o.d.) with their tips separated by about 3 cm along the length. Cylindrical Pb-Sb alloy plugs were placed at the bottom end of the quartz ampoules. These plugs had axial holes through which the silica capillaries containing the thermocouples were inserted into the quartz ampoule. The quartz ampoule was then sealed at the bottom. It was evacuated from the top and heated in the directional solidification furnace to create a 15- to 20-cm-long melt column that fused with the preexisting Pb-Sb alloy plug at the bottom. Directional solidification was carried out by withdrawing the ampoule from the furnace assembly at various speeds. Temperature profiles within the specimens were recorded by the two thermocouples during translation. Steady-state thermal profile was maintained, as indicated by identical thermal profiles obtained from the two thermocouples. After 10 to 12 cm of directional solidification, the ampoule was quickly withdrawn from the furnace and the melt column quenched by spraying water on the ampoule surface. The thermal gradient in the liquid at the liquid-solid interface during these experiments was observed to be $140 \pm 8 \text{ K cm}^{-1}$.

Longitudinal and transverse microstructures were examined in the unetched condition by standard optical metallography techniques. Two-millimeter-thick slices were machined as a function of distance along the length of the directionally solidified specimens. These were analyzed for their antimony content (C_s) by the "wet" chemistry technique, atomic absorption spectroscopy, to examine the longitudinal macrosegregation. The ratio of the distance solidified to the initial melt column length is taken as the fraction solidified (f_s).

III. RESULTS

Figure 1 shows typical longitudinal microstructure of the directionally solidified Pb-5.8 wt pct Sb alloy at the quenched liquid-solid interface. With increasing growth

S.N. OJHA, formerly Visiting Professor, Chemical Engineering Department, Cleveland State University, is Professor, Department of Metallurgical Engineering, Banaras Hindu University, Varanasi, India 221-005. G. DING, Research Associate, Y. LU, Graduate Student, J. REYE, Undergraduate Student, and S.N. TEWARI, Professor, are with the Chemical Engineering Department, Cleveland State University, Cleveland, OH 44115.

Manuscript submitted September 9, 1998.

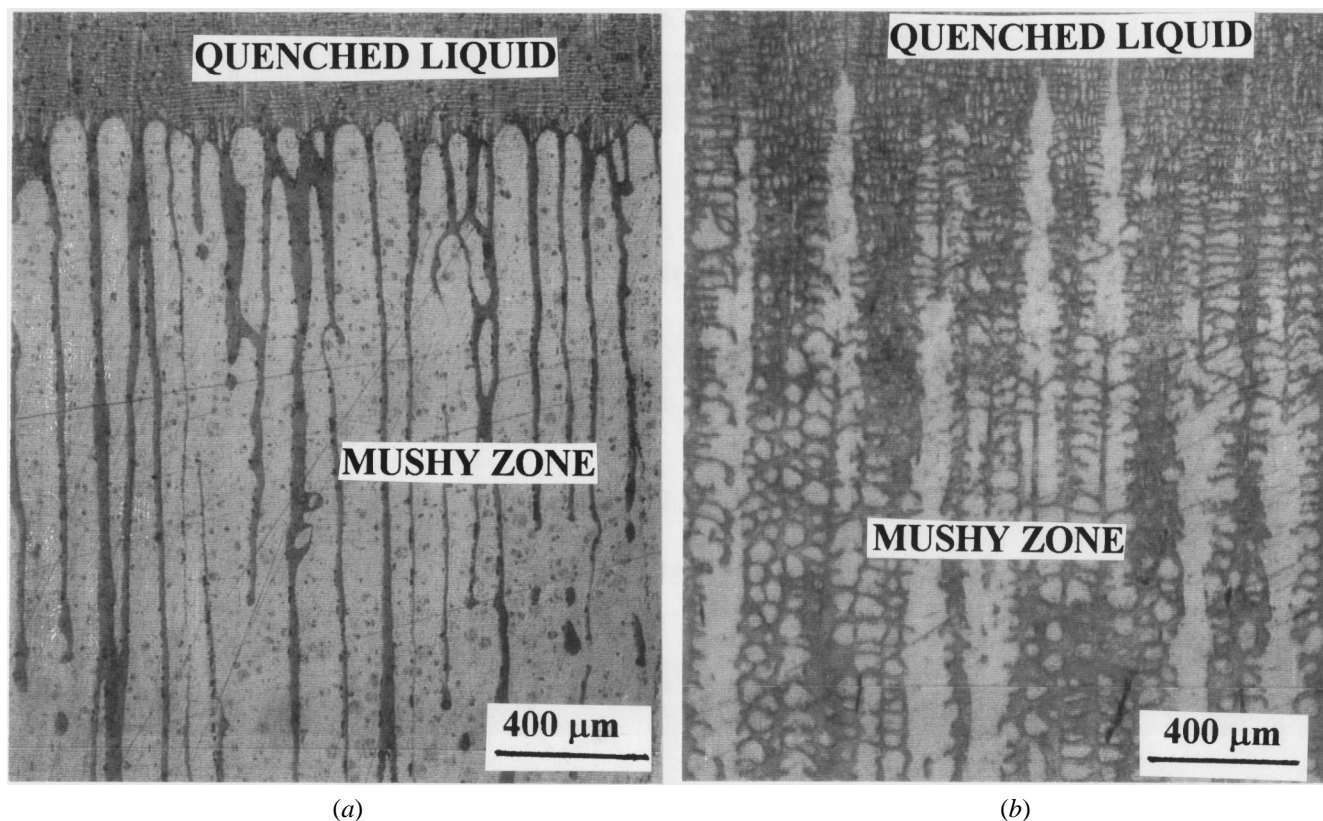


Fig. 1—Typical longitudinal microstructures of directionally solidified Pb-5.8 wt pct Sb alloy near the quenched cellular/dendritic array tips: (a) cellular array ($V = 0.8 \mu\text{m s}^{-1}$) and (b) dendritic array ($V = 3.0 \mu\text{m s}^{-1}$).

speed, the microstructure changed from planar to cellular to dendritic. For the Pb-5.8 wt pct Sb alloy, the microstructures were cellular for growth speeds less than $1.5 \mu\text{m s}^{-1}$ and dendritic for higher growth speeds. For the Pb-2.2 wt pct Sb alloy, this transition occurred at $3.5 \mu\text{m s}^{-1}$. Examination of the longitudinal sections near the quenched array tips showed that the cells and dendrites were aligned parallel to the alloy growth direction. The eutectic isotherm in the longitudinal microstructure was clearly identifiable because of the change in the interdendritic solid morphology, from an aligned two-phase eutectic-composite-like morphology at temperatures below the eutectic temperature to the random two-phase distribution in the quenched mushy zone above it. The mushy-zone length was constant across the entire specimen cross section, indicating the absence of any significant transverse temperature gradient in the melt. The distribution of the cells or dendrites was uniform across the entire specimen cross section. Similar microstructures were observed for the directionally solidified Pb-2.2 wt pct Sb alloy.

Typical growth-speed dependence of the longitudinal macrosegregation for the directionally solidified Pb-Sb alloys is shown in Figure 2, which plots C_s/C_o vs fraction solidified (f_s); C_s being the antimony content at f_s , and C_o being the original antimony content of the melt. In this figure, the symbols marked by “L” correspond to the quenched liquid portion of the specimens. For each directionally solidified specimen, the C_o values obtained by measuring the area under the C_s vs f_s plots, which included both the directionally solidified and quenched melt portions, was found to be within ± 5 pct of the analysis obtained from the

specimens cut from the precast feedstock bars. Figure 2(a) corresponds to the Pb-2.2 wt pct Sb and Figure 2(b) corresponds to the Pb-5.8 wt pct Sb alloy. These figures show that C_s/C_o increases from less than unity to values larger than unity as a function of f_s . In the absence of convection, a uniform solute content will be expected along the length of the directionally solidified dendritic/cellular specimens, except for the initial and final transients (with lengths about the size of the mushy-zone length). Data for one Pb-5.8 wt pct Sb cast feedstock sample that was similarly analyzed along the specimen length and did not show any longitudinal macrosegregation have not been included in this figure for the sake of clarity. The extent of macrosegregation increases with decreasing growth speed for both alloys. The cellular specimens grown at lower growth speeds show larger macrosegregation as compared with the dendritic specimens solidified at higher growth speeds. Similar observations in hypoeutectic Pb-Sn alloys were reported.^[5]

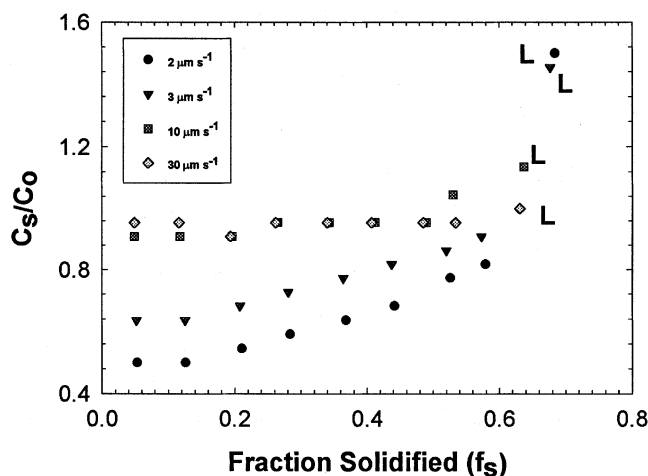
IV. DISCUSSION

A. Effective Partition Coefficient

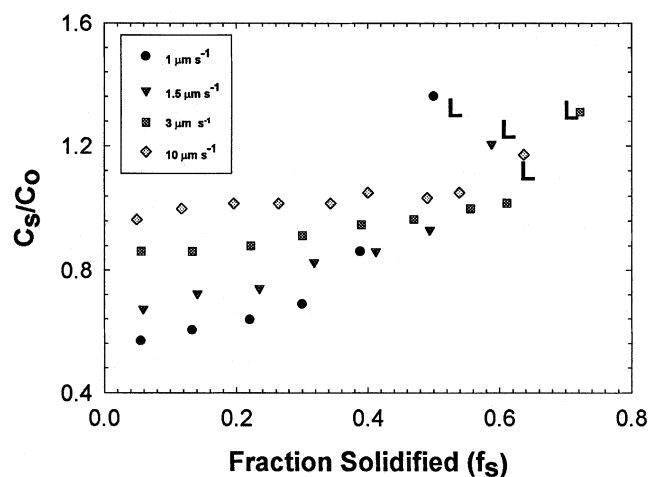
Macrosegregation in the presence of convection during directional solidification with a planar liquid-solid interface is described as follows by the Burton-Prim-Slichter (BPS)^[8] relationship:

$$C_s = k_e C_o (1 - f_s)^{k_e - 1} \quad [1]$$

where k_e is the effective solute partition coefficient corresponding to a solutal boundary-layer thickness δ in the melt^[8]



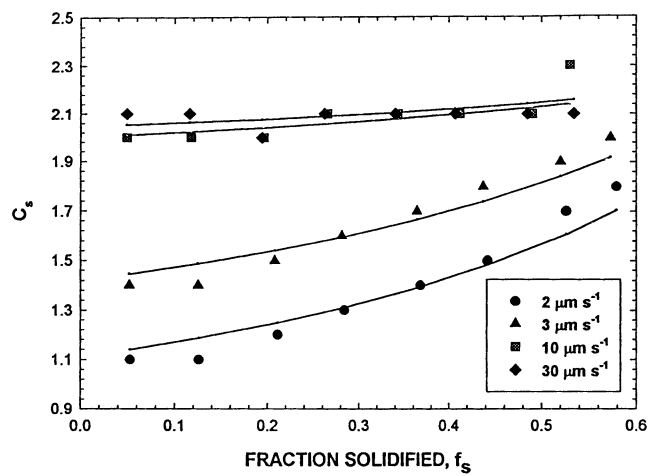
(a)



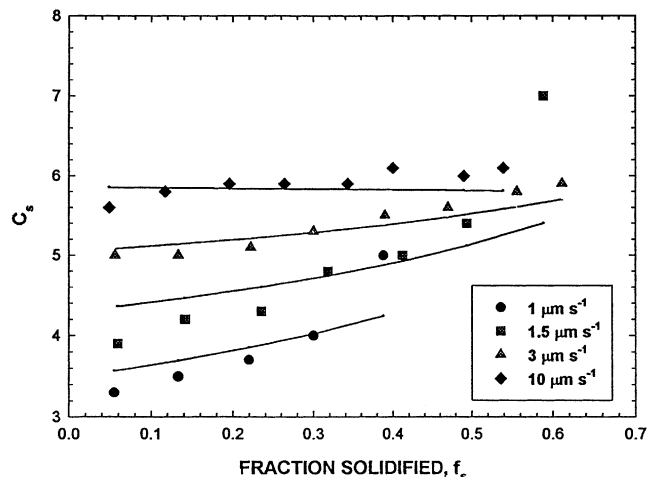
(b)

Fig. 2—Influence of growth speed on macrosegregation along the length of directionally solidified Pb-Sb alloys ($G_I = 140 \text{ K cm}^{-1}$): (a) Pb-2.2 wt pct Sb and (b) Pb-5.8 wt pct Sb.

ahead of a planar liquid-solid interface. The k_e in the BPS relationship is also the ratio of the solute content of the solid at the liquid-solid interface (C_s) at any given instant and the corresponding solute content of the bulk melt (C_l). This approach assumes a complete mixing in the melt and diffusive mass transport through the boundary-layer thickness. As the extent of convection increases from purely diffusive mass transport toward complete mixing in the melt, the effective partition coefficient decreases from nearly unity to k , the equilibrium partition coefficient from the phase diagram. Because of the lack of a similar rigorous analysis, it has been assumed that the aforementioned relations are also valid for the cellular/dendritic morphologies.^[5,9] For a cellular/dendritic arrayed growth, there is no sharp boundary between the completely liquid and completely solid regions. One can, however, visualize that the sharp planar liquid-solid interface of the BPS relationship is now replaced by a diffused boundary, the mushy zone. There is complete liquid on top of the array tips and complete solid below them. Hence, the ratio of the solute content of the directionally solidified portion just below the quenched mushy zone to that of the quenched melt (C_q) would be akin to the C_s/C_l ratio in the BPS relationship.



(a)



(b)

Fig. 3—Nonlinear regression analysis of the longitudinal macrosegregation data to obtain effective partition coefficient (k_e) from $C_s = k_e C_o(1 - f_s)^{k_e - 1}$. (a) Pb-2.2 wt pct Sb and (b) Pb-5.8 wt pct Sb.

A single-parameter, nonlinear regression analysis, using SIGMASTAT,^[10] has been used to obtain k_e by fitting the C_s vs f_s data shown in Figure 2 (excluding the quench liquid portion of the data) to the relationship presented in Eq. [1]. The result is shown in Figure 3, where the solid lines are the fitted curves. This regression analysis provided a very good fit with the macrosegregation data for the Pb-2.2 wt pct Sb alloy (Figure 3(a)). The fit for the Pb-5.8 wt pct Sb alloy is also good (Figure 3(b)), except for the two data points at the highest f_s values for the samples grown at 1 and $1.5 \mu\text{m s}^{-1}$.

Figure 4 compares the k_e values obtained from the regression fit of C_s vs f_s data and those obtained from the ratio of the antimony content of the directionally solidified portion just below the quenched mushy zone to the antimony content of the quenched melt (C_q). The error bars in this figure correspond to one standard deviation in the effective partition coefficient that was obtained from the nonlinear regression fit. The effective partition coefficients obtained by the two methods are almost identical for all the growth conditions examined in this study. This observation, analogous to the macrosegregation in the presence of convection for a planar

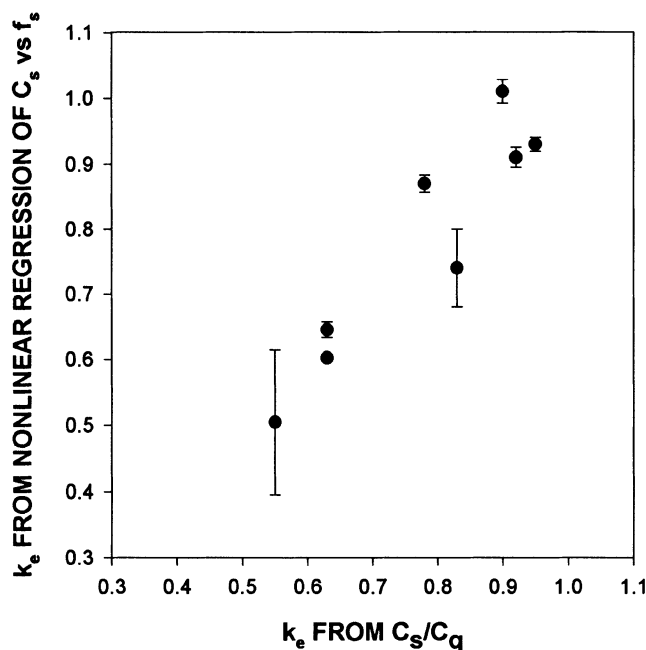


Fig. 4—Comparison of the effective partition coefficients obtained by nonlinear regression analysis of the longitudinal macrosegregation data and by taking the ratio of the solid and liquid compositions at quench.

liquid-solid interface, further supports the use of this parameter, the effective partition coefficient, to indicate the extent of longitudinal macrosegregation during directional solidification with a cellular/dendritic liquid-solid interface. Lower growth speeds, which correspond to cellular morphologies, have larger macrosegregation and yield low k_e , about 0.5. Higher growth speeds produce dendritic morphologies, less macrosegregation, and yield k_e values approaching unity. In the following sections, we will use the average of the two k_e values; *i.e.*, that obtained from the nonlinear regression analysis of the C_s vs f_s data and that obtained from the C_s to C_q ratio.

B. Convection Due to Solutal Buildup at Dendrite Tips

Temperature and composition profiles in the melt near the tips of the primary dendrite array, both in the interdendritic mushy region and in the bulk melt ahead of the array, for directional solidification of a hypoeutectic Pb-Sb alloy are schematically shown in Figure 5. The figure also contains the Pb-Sb phase diagram. During directional solidification, the mushy zone contains lead-rich primary cells/dendrites. The antimony content of the melt decreases from the eutectic (11.2 wt pct Sb) at the base of dendrites to the tip composition, C_t , at the dendrite tips. The solute content of the bulk liquid decreases from C_t to the melt composition, C_o , over a characteristic distance equal to D_l/V , where, D_l is the solutal diffusivity in the melt and V is the growth speed. Increasing antimony content in the melt leads to a decreasing melt density. Therefore, during directional solidification with the melt on top and solid below, with gravity pointing down, the density profile in the interdendritic melt and in the melt immediately ahead of the tips promotes natural convection (higher density melt on top of that with lower density). For dendritic morphologies (observed at larger growth speeds),

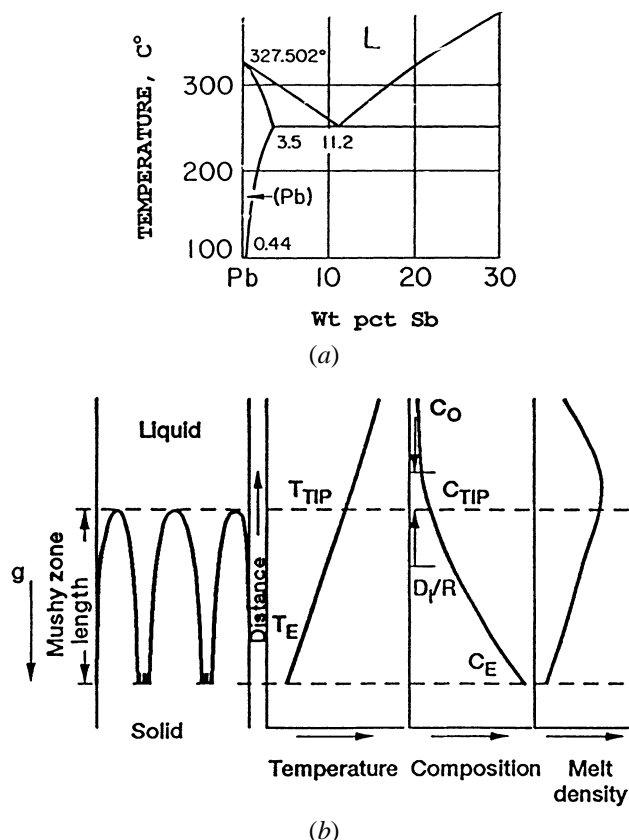


Fig. 5—(a) Pb-Sb phase diagram. (b) Schematic temperature, composition, and density profiles in the mushy region and in the overlying melt ahead of the cellular/dendritic array during directional solidification of hypoeutectic Pb-Sb alloys.

the solutal buildup at the tip is expected to be minimal. The interdendritic density profile, therefore, plays a crucial role in determining the extent of natural convection. However, the solute buildup at the tip is much larger for the cellular arrays that form at lower growth speeds. This not only produces a larger density inversion in the melt ahead of the tips at lower growth speeds, but the inversion also exists over a larger distance. Thermosolutal convection in the bulk melt is, therefore, very important for the cellular morphologies. Convection near the tips also entrains into the mushy region, which results in the longitudinal (parallel to the growth direction) and transverse macrosegregations.

C. Longitudinal Macrosegregation and Thermosolutal Convection

A dimensionless parameter, the Grashoff number ($G_r = g(\delta\rho/\rho)(H^3/\eta^2)$), has been used in the literature to describe the relative influence of the buoyancy and viscosity in natural convection.^[11] Here, g is the gravitational acceleration, η is the kinematic viscosity, and $(\delta\rho/\rho)$ is the relative fluid density change over the characteristic distance, H . For $G_r \gg 1$, the fluid velocity has been estimated to be equal to $[g(\delta\rho/\rho)H]^{1/2}$.^[11] The characteristic distance for this study is best represented by D_l/V because the thermosolutal convection is primarily caused by the solute buildup at the array tips. The fluid velocity is therefore expected to be proportional to $[g(C_t - C_o)D_l/VC_o]^{1/2}$. Higher fluid velocities (more intense

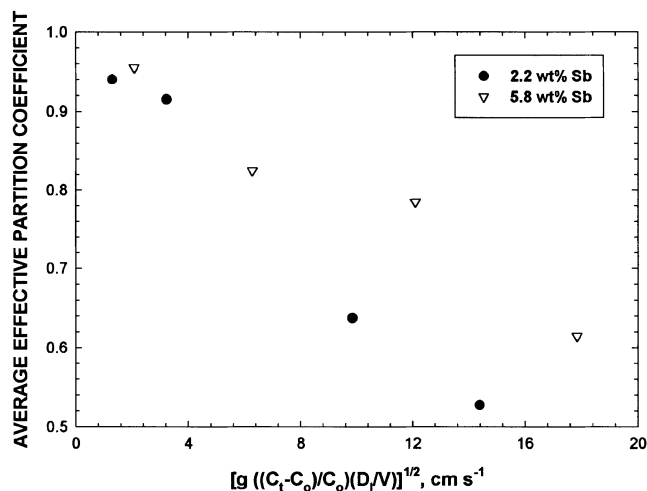


Fig. 6—Correlation between the extent of longitudinal macrosegregation as indicated by the effective partition coefficient and the parameter $[g(C_t - C_o)D_l/VC_o]^{1/2}$, which represents the extent of convection caused by the build up of low density solute at the tips of cellular/dendritic arrays during directional solidification of hypoeutectic Pb-Sb alloys.

convection) will result in larger longitudinal macrosegregation indicated by smaller k_e .

Figure 6 plots the experimentally observed average k_e vs $[g(C_t - C_o)D_l/VC_o]^{1/2}$. The C_t values used in this figure are the ones predicted from the Hunt–Lu model^[12] (which does not include convection in its analysis) for the given growth parameters and the alloy physical properties. This figure shows that the larger fluid velocities, expected with increasing $[g(C_t - C_o)D_l/VC_o]^{1/2}$, also result in increased longitudinal macrosegregation, as indicated by the k_e values decreasing from unity.

V. CONCLUSIONS

The following conclusions can be drawn from this study on the longitudinal macrosegregation in hypoeutectic Pb-Sb alloys directionally solidified with a cellular/dendritic array morphology.

1. Thermosolutal convection caused by the buildup of low-density solute ahead of the growing arrays of cells and dendrites produces macrosegregation along the solidified length. The parameter $[g(C_t - C_o)D_l/VC_o]^{1/2}$, where C_o is the solute content of the alloy, C_t is the melt composition at the array tip, D_l is the solute diffusivity, and V is the growth speed, can be used to describe the intensity of this convection.
2. The extent of macrosegregation is quantitatively represented by the parameter k_e (the effective partition coefficient), which is about unity in the absence of convection and decreases with the increasing convection.
3. Cellular morphologies growing at smaller growth speeds have larger C_t values, more intense convection, and, therefore, larger macrosegregation as compared with dendrites.

ACKNOWLEDGMENTS

Support for this research was provided by NASA–Microgravity Science and Applications Division and NASA–Marshall Space Flight Center.

REFERENCES

1. J.R. Sarazin and A. Hellawell: *Metall. Trans. A*, 1988, vol. 19A, pp. 1861-71.
2. C.F. Chen and F. Chen: *J. Fluid Mech.*, 1991 vol. 227, pp. 567-86.
3. H.W. Huang, J.C. Heinrich, and D.R. Poirier: *Modelling Simul. Mater. Sci. Eng.*, 1996, vol. 4, pp. 245-59.
4. M.H. Burden, D.J. Hebditch, and J.D. Hunt: *J. Cryst. Growth*, 1973, vol. 20, pp. 121-24.
5. S.N. Tewari, R. Shah, and M.A. Chopra: *Metall. Trans. A*, 1993, vol. 24A, pp. 661-1669.
6. S.N. Tewari and R. Shah: *Metall. Trans. A*, 1992, vol. 23A, pp. 3383-92.
7. S.N. Tewari and R. Shah: *Metall. Mater. Trans. A*, 1996, vol. 27A, pp. 1353-62.
8. J.A. Burton, R.C. Prim, and W.P. Slichter: *J. Chem. Phys.*, 1953, vol. 21, pp. 1987-91.
9. J. Verhoeven: *Metall. Trans.*, 1971, vol 2, pp. 673-80.
10. "SIGMASTAT" is a statistical analysis software by SPSS Inc., 444 North Michigan Avenue, Chicago, IL 60611.
11. S.M. Pimputkar and S. Ostrach: *J. Cryst. Growth*, 1981, vol. 55, pp. 614-46.
12. J.D. Hunt and S.Z. Lu: *Metall. Mater. Trans. A*, 1996, vol. 27A, pp. 611-23.